TRANSVERSE IMPACT OF CIRCULAR MARINE COMPOSITE PLATES

Sutherland, L.S.[1] and Guedes Soares, C.[2]

[1] Bolseiro de Pós-Doutoramento, [2] Prof. Catedrático,
Unidade de Engenharia e Tecnologia Naval, IST, Av. Rovisco Pais, 1049-001 Lisboa, Portugal
+351 218 417 468 / uetn@mar.ist.utl.pt

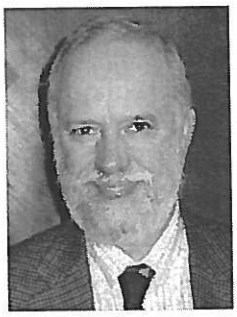

ABSTRACT

Falling-weight impact tests on circular low fibre-volume E-glass / polyester composite plates have been performed. Three behaviour 'regimes' have been defined: 'Undelaminated', 'Delaminated' and 'Fibre damage'. A fracture mechanics model describes extremely well the sudden onset of delamination, and gives good scaling between specimen sizes. Bending and membrane effects are significant for thin laminates. For thick laminates, especially after the sudden onset of delamination, the response is shear-dominated. Delaminated behaviour was well described by an energy balance model. Final failure appears to be due to back-face strains.

1. INTRODUCTION

The use of composite materials in a marine environment is advantageous due to their ease of forming double-curvatures, resistance to corrosion and rot, and high specific material properties. However, a known disadvantage of these materials is that they are susceptible to impact damage, especially that due to out of plane impact. This disadvantage is exacerbated by the fact that the behaviour under impact loading is not well understood, and this lack of confidence often leads to increased safety factors and loss of potential weight savings. Mouritz et al (2001) quote safety factors of up to 10 applied when marine composite structures will be subjected to impact loads. In a marine environment, common impact events are collisions with other craft, docks, floating debris and grounding, all of which are low-velocity impacts.

The response of a composite material to impact is highly complex involving not only dynamic effects but also numerous and interacting damage modes including internal delamination, surface micro buckling, fibre fracture and matrix degradation (Richardson and Wiseheart, (1996)). The impact behaviour and the damage modes and paths are themselves dependant in a complex manner on the almost infinite material permutations including fibre and resin types, quantities, architectures, and interface and on the production method used (Cartié and Irving (2002), Caprino and Lopresto (2001), Hirai et al. (1998)).

It is also difficult to use the term 'impact response' as it is possible to define the

tensile, compressive or bending behaviour of a composite material since the impact event is defined by many variables such as impacter and target geometries, impact speed and energy (Christoforou (2001), Sutherland and Guedes Soares (2003)).

Hence, there has been a large amount of work in the area. Abrate (1998) provides both a comprehensive review and a classification of the different areas of the problem. The analysis of the behaviour of an impacted laminate is usually split into two parts; the localised contact problem and the overall target deflection. Hertzian contact law is usually used to model indentation at the surface (e.g. Sun et al. (1993), Yang and Sun (1982)). Complete models may be used to exactly describe the deformation of the target using beam or plate theories (e.g. Chen and Sun (1985)) for simple cases for small deflections.

However, these models rapidly become too computationally expensive when considering more complex architectures, large deflections or cases with significant shear deformations. They are also not effective for the consideration of damage. A more approximate and realistic approach in these latter cases is to use theories to describe the overall response of the composite such as the energy balance and spring-mass methods as described in Abrate (2001), where a concise overview of all of the main modelling techniques used may also be found.

The majority of the work in the area concerns the high-cost, high fibre-fraction, usually pre-impregnated carbon-fibre epoxy based autoclave or vacuum-bag produced composites associated with the aerospace materials. However, the composite materials used in the marine industry are much lower fibre-faction, hand laid-up glass-reinforced polyester resins and there is very little data available concerning these lower cost composites.

Previous work (Sutherland and Guedes Soares (1999a and b)) considered the low-energy impact of such marine composites. Specifically, the out of plane, central impact of a clamped rectangular plate with a small, steel hemispherical impacter was considered as a relatively severe case. Here the aim is to further this work by studying the impact of theoretically simpler circular plates and hence to further characterise the various impact damage mechanisms occurring.

2. EXPERIMENTATION

Flat panels of 1m by 1m were laminated by hand using orthophthalic polyester resin and 500gm^{-2} E-glass balanced woven roving. A fibre mass-fraction of 0.5 (equivalent to a fibre volume fraction of approximately 0.35) was stipulated as representative of that commonly achieved under production conditions in the marine industry. 1, 2 and 3% by mass of accelerator, catalyst and paraffin respectively were used, in an ambient temperature of between 18 and 21 degrees Celsius, to cure the resin. In order to ensure a full cure, all specimens were stored at room temperature for four months before testing.

Specimens were cut from the panels using a diamond-surrounded circular saw. Panels of 3, 5, 10, and 15 plies were cut into 'Small' 100mm square specimens. 'Large' 200mm square specimens were cut from panels of 5, 10, 15 and 20 plies. Four thickness measurements were made on each specimen before testing.

A fully instrumented Rosand IFW5 falling weight machine was used for the impact testing (Figure 1). A hemispherical ended cylindrical impacter is dropped from a known, variable height between guide rails onto a clamped horizontally supported plate target. A much larger, variable mass is attached to the impacter and a load cell between the two gives the variation of impact force with time. The data was filtered with a 2kHz low pass filter. An optical gate gives the incident velocity, and hence the impacter displacement and velocity and the energy it imparts are calculated from the force-time data by successive numerical integrations. Since the

impacter is assumed to remain in contact with the specimen throughout the impact event, the impacter displacement is used to give the displacement and velocity of the top face of the specimen, under the impacter. By assuming that frictional effects are negligible, the energy imparted by the indenter is that absorbed by the specimen. Thus, this energy value at the end of the test is that irreversibly absorbed by the specimen.

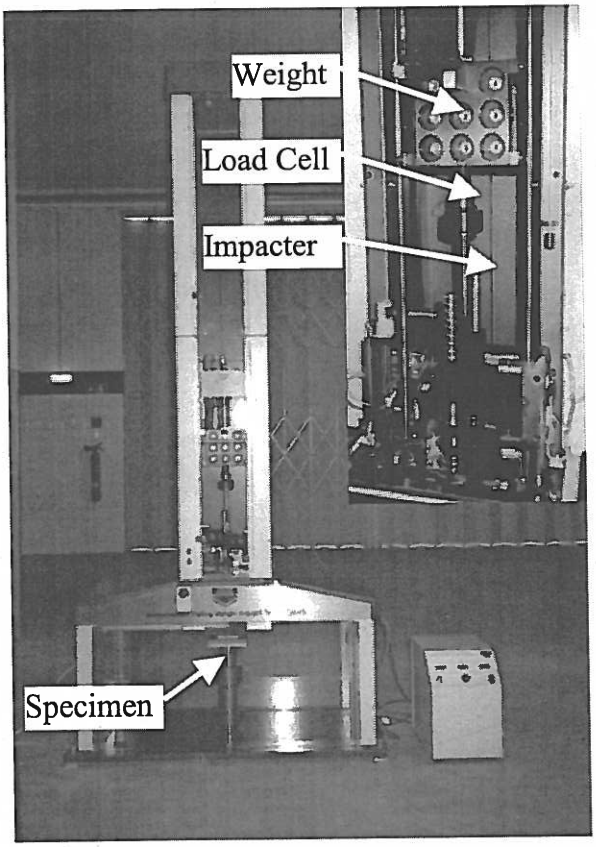

Fig 1: Falling Weight Impact Machine

The specimens were fully clamped between two thick annular circular steel plates. The clamping force was applied using a pneumatic actuator and a long lever arm to achieve high forces. The 'small' and 'large' specimens were tested using clamps with inside diameters of 50mm and 100mm respectively. A 10mm and a 20mm diameter impacter were used to strike the small and large specimens respectively.

Tests were performed for a range of increasing incident energies either up to perforation where possible, or to the maximum attainable by the machine. Nominally the impact masses used were 2.853kg and 10.853kg for the small and large specimens respectively, but the mass used for the some of the higher incident energy impacts of the small specimens was increased to give perforation at the maximum velocity attainable. After testing the damage modes were observed and noted.

3 RESULTS

Damage occurred at all but the very lowest incident energies, including matrix cracking, matrix degradation, permanent indentation, internal delamination, partial surface micro-buckling delamination of the upper 'front-face' laminate, front-face fibre damage, fibre damage on the lower 'back-face', and perforation. These modes form a complex overall damage pattern, but the progression of damage with increasing incident energy is similar for all specimens:

1. *'Un-delaminated'*: At extremely low incident energies damage is slight and mainly restricted to matrix cracking.
2. *'Delaminated'*: At a low critical incident energy delaminations suddenly appear, which then spread with increasing impact severity.
3. *'Fibre Damage'*: At higher energies fibre failure occurs, leading to perforation.

Importantly, since the damage seen is directly responsible for the behaviour seen, these definitions also allow simple characterisation of the impact response. However, some differences in damage were seen between 'thin' and 'thick' specimens (in this case diameter to thickness ratios of greater than and less than 15 respectively) as illustrated in Figures 2 and 3 (where the front-face is shown above the bottom-face). The main differences were that the thinner specimens incurred much less internal delamination, but were more prone to back face fibre damage.

The impact response also differs between thin and thick specimens as shown in the force-displacement and force-time plots Figures 4 and 5. Each graph shows a family of curves for increasing incident energy.

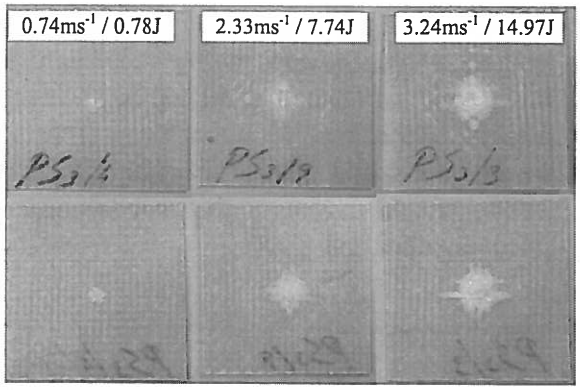

Fig 2: Impacted Thin Laminates (3-ply 50mm Diameter)

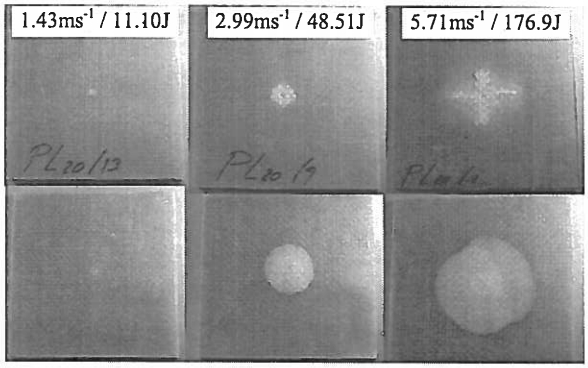

Fig 3: Impacted Thick Laminates (20-ply 100mm Diameter)

Thinner laminates show the increase in stiffness with displacement due to membrane effects until fibre damage gives a sharp drop in force. Thicker laminates show a bi-linear response due to the onset of internal delamination. Despite the fact that internal delamination also occurred in the thinner laminates, no effect of this is seen in Figure 4.

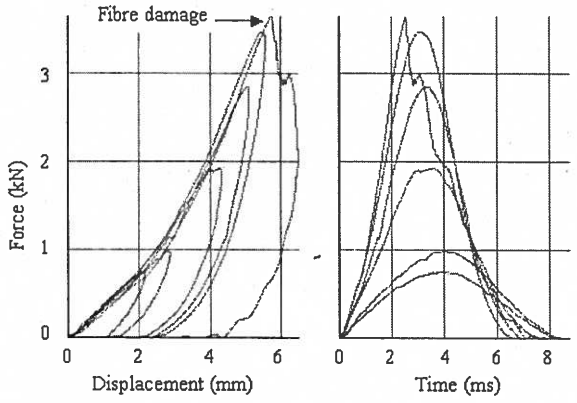

Fig 4: Impact Response Thin Laminate

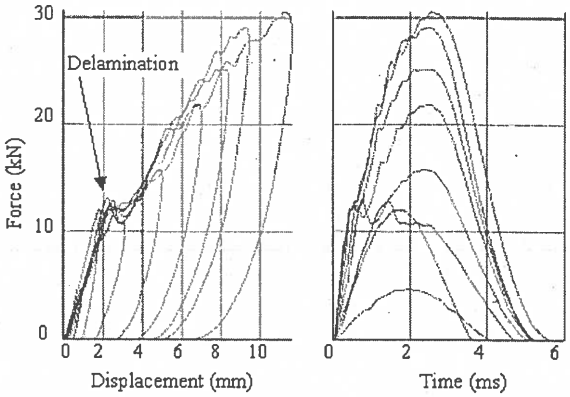

Fig 5: Impact Response Thick Laminate

4 ANALYSIS

4.1 Indentation

The geometry of the impact event is defined in Figure 6. The measured *displacement* of the impacter (δ) is made up of the sum of the plate *deflection* (w) and the *indentation* (α).

i.e. $$\delta = w + \alpha \qquad (1)$$

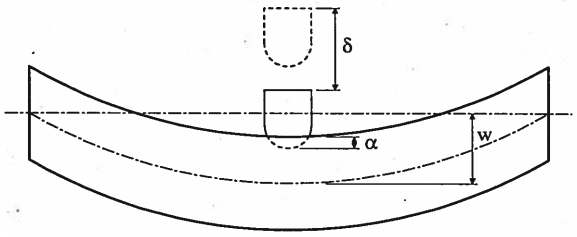

Fig 6: Impact Geometry

The Hertzian contact law relates the contact force P to the indentation. For a rigid spherical indenter and a transversely isotropic half-space this may be expressed as (Tan and Sun (1985)):

$$P = k\alpha^{3/2} \qquad (2)$$

where k is a contact coefficient depending on target and sphere material properties, and the sphere radius. Complementary work (Sutherland et al (2004)) has shown this to be the case at lower contact forces, but then as contact damage occurs the relationship becomes linear. The experimental data from the indentation

work was used here to obtain the plate deflections from the displacement data.

4.2 Internal Delamination

Internal delamination is the first damage leading to a significant reduction in material properties. It is important to predict the onset of this since a pigmented gel coat or paint covering will hide such damage in practice. Such damage gives a local stiffness reduction, which may cause a future failure when an abnormally large loading is encountered and/or the damage grows with cyclic loading. The fact that delamination occurs here at such low incident energies indicates that many vessels will have considerable undetected delamination due to even minor, everyday impacts.

Davies et al (1993) use a simple mode II fracture analysis to describe the critical load for the unstable onset of a single circular delamination in an isotropic material:

$$P_c = \frac{2\sqrt{2\pi}}{3}\left(\frac{EG_{IIc}}{1-\nu^2}\right)^{1/2} h^{3/2} \qquad (3)$$

where E is Young's modulus, G_{IIc} is the mode II strain energy release rate, ν is Poisson's ratio, and h is laminate thickness. Davies and Zhang (1995) used this approach fairly successfully for carbon epoxy, but satisfactory results were not obtained for high fibre-volume fraction glass polyester laminates (Zhou and Davies (1995)). Cartié and Irving (2002) obtained such good correlation using this method for CFRP that they advocated the use of impact testing to determine G_{IIc}. Christoforou (2001) also used equation (3) to define the onset of delamination.

A logarithmic plot of P_c against h for the tests carried out here is made in Figure 7. The data fits the theory extremely well, as shown by the high 'goodness of fit' R^2 value, although the slope is slightly higher than the theoretical value of 1.5. Importantly, the theory scales extremely well between the small and large specimens. The static values shown are from quasi-static replications of the impact set-up. Again very good correlation with the theory is shown, with delamination occurring at a slightly lower force than for the impact tests. This indicates that the use of far simpler quasi-static testing may provide a practical, if slightly conservative, data for internal delamination due to impact.

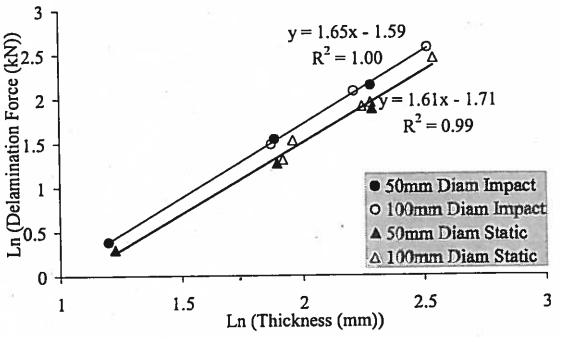

Fig 7: Delamination Threshold

4.3 Plate Deflections

Here both large deflections of thin plates where membrane effects become important, and also deflections of thick plates where the effects of shear must be considered. Shivakumar et al, 1985 provide the relationship between impact force P and plate deflection w in terms of bending, shear and membrane stiffness (K_b, K_s and K_m respectively) for a centrally loaded circular plate:

$$P = K_{bs} w + K_m w^3 \qquad (4)$$

$$K_{bs} = \frac{K_b K_s}{K_b + K_s} \qquad (5)$$

Expressions for the stiffness are also given for the four permutations of clamped or simply supported specimens with immovable or movable edges. These may be expressed in the form:

$$K_m = A_o h; \quad K_b = B_o h^3; \quad K_s = C_o h \qquad (6)$$

where h is laminate thickness, A_o, B_o and C_o are constant for a given material and plate

diameter, and in the case of Co, assuming the contact area a_c is constant.

Here the aim is to present the data in such a form that it is possible to separate and characterize the various impact mechanisms occurring. Based on the results of previous work (Sutherland (1999b)) the response will be assumed to be shear controlled and then deviations from this simplified model will be used to distinguish the various types of behaviour.

Firstly, assuming that membrane effects are negligible and combining equations (4), (5) and (6) gives:

$$\frac{P}{h} = C_o \left(\frac{h^2}{h^2 + C_o / B_o} \right) w \qquad (7)$$

Hence, if membrane effects are not significant, plots of P/h against w for different specimen thickness will give linear relationships whose slopes increase with thickness (for a given material and plate diameter). For very thick laminates shear deflections dominate and equation (7) may be further simplified to give:

$$\frac{P}{h} = C_o w \qquad (8)$$

Hence, if shear deflections dominate, plots of P/h against w for different specimen thickness will give linear relationships whose slopes are independent of thickness. In Figures 8 and 9 the maximum force normalized by thickness is plotted against the corresponding plate deflection for each test. In all graphs that follow points containing a cross indicate no delamination and those containing a dot indicate fibre failure.

The thinnest specimens show stiffening with increased deflection due to membrane effects. A bi-linear response is seen for the thicker specimens, indicating that membrane effects are not significant in these cases. A stiffer undelaminated response is followed by a less stiff delaminated response. For the undelaminated response the stiffness increases with thickness, but is approaching a constant value for the thickest specimens, indicating that shear deflections dominate for thicker specimens even before delamination. After delamination the thicker specimens are approximately equally stiff, indicating that shear deflections dominate the delaminated behaviour.

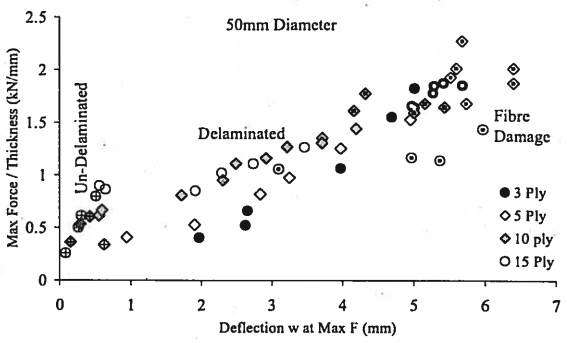

Fig 8: Small Specimens Maximum Force

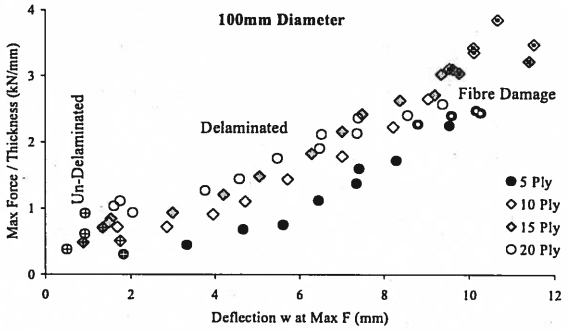

Fig 9: Large Specimens Maximum Force

4.4 Energy Balance

In order to characterise the relationship between the severity of the impact event and the force-deflection behaviour an energy balance approach is taken. At the maximum deflection the specimen absorbs all of the incident energy.

Calculating the energy absorbed by integration of the force-deflection response, noting that for all tests where fibre damage is not significant the maximum force and maximum deflection occur almost simultaneously, and normalising both sides by thickness gives:

$$\frac{IKE}{h} = \int_0^{w_{P\,Max}} \frac{P}{h} dw \qquad (9)$$

Again, shear deflections are assumed to dominate and then deviations from this behaviour used to identify the different mechanisms. The force-deflection behaviour for thicker specimens was bi-linear (Figure 5), and equation (8) may be modified accordingly:

$$\frac{P}{h} = C_0 w \quad for\ w \le w_C \quad (a)$$
$$\frac{P}{h} = C_1 w + (C_0 - C_1) w_C \quad (b) \qquad (10)$$
$$for\ w \ge w_C$$

where C_0 and C_1 are the 'thickness-normalised stiffness' of the un-delaminated and delaminated behaviours respectively and w_c is the deflection corresponding to P_c. Substituting for P/h from equations (10) into equation (9), integrating and then using equations (10) to express the result in terms of maximum force gives the bi-linear relationship:

$$\left(\frac{P_{Max}}{h}\right)^2 = 2C_o\left(\frac{IKE}{h}\right) \quad (a)$$
$$for P \le P_C \qquad (11)$$
$$\left(\frac{P_{Max}}{h}\right)^2 = 2C_1\left(\frac{IKE}{h}\right) + \left(\frac{C_o - C_1}{C_o}\right)\left(\frac{P_C}{h}\right)^2 \quad (b)$$
$$for P \ge P_C$$

In Figures 10 and 11 $(P_{Max}/h)^2$ is plotted against IKE/h. In both graphs the un-delaminated behaviour forms only a small initial part of the response. The upward-curving trend of the thinnest specimens due to membrane effects is again evident. However, the main point is that the data collapses very nicely onto a common linear trend for the delaminated case.

4.5 Fibre Damage

For the highest IKE test in Figure 4 the displacement increases, as fibres are broken, after the maximum load has been reached. That is, the maximum load and displacements no longer occur simul-taneously. Hence, the difference between

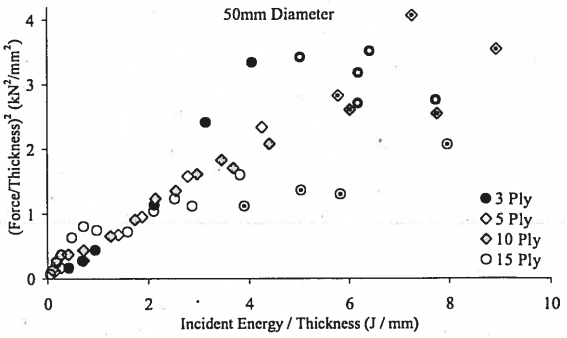

Fig 10: Small Specimens Energy Balance Plot

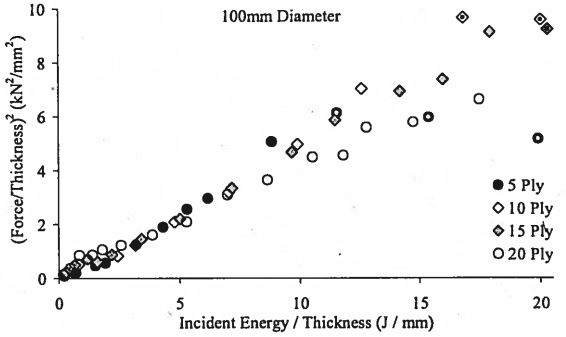

Fig 11: Large Specimens Energy Balance Plot

the maximum displacement and the displacement at maximum force is used here as an indicator of the onset of fibre damage.

Perforation could be initiated by one of two plausible damage paths; bending giving back-face fibre tensile failure, and high contact forces giving front-face fibre 'shear-out' failure. If the former is the controlling mechanism then fibre failure should occur at a critical plate deflection for a given plate diameter. Conversely, if the latter initiates perforation then fibre failure should occur at a critical contact force, independent of plate diameter. Figures 12 and 13 indicate that the start of fibre failure is bending controlled since this starts at an approximately constant deflection. However, Figure 14 shows that fibre failure of the small 10-ply and 15-ply specimens occurs at approximately the same maximum force. This provides some, but inconclusive, evidence that contact force initiates perforation for the thickest laminates.

4.6 Impact Duration

A spring-mass model approach assuming geometrical non-linearities and indentation are negligible gives the result for contact time T_C as (Abrate 1998):

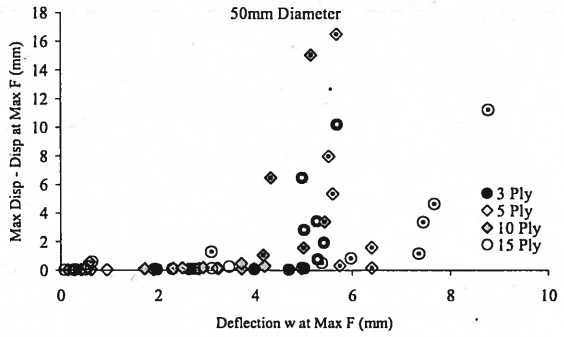

Fig 12: Fibre Damage Parameter vs. Deflection, Small Specimens

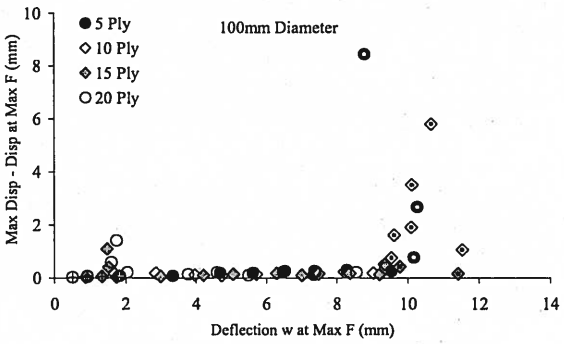

Fig 13: Fibre Damage Parameter vs. Deflection, Large Specimens

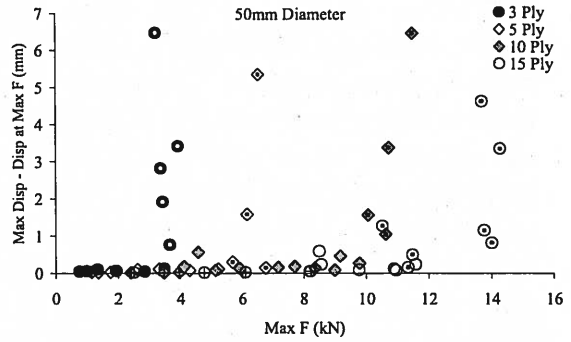

Fig 14: Fibre Damage Parameter vs. Maximum Force, Small Specimens

$$T_C = \pi (M / K_{bs})^{1/2} \qquad (12)$$

Hence, the impact duration should be independent of incident energy, increase with impacter mass M but decrease with increasing stiffness K_{bs}. Damage will extend the impact event. Figures 15 and 16 show the durations of the impacts of the small and large specimens respectively. All but the thinnest specimens show an increase in impact duration as delamination occurs. This is followed by fairly constant impact durations for the delamination-controlled behaviour, until the impact event is further prolonged by fibre damage. In the case of the thickest specimens the undelaminated behaviour is reflected by an approximately constant duration at low IKE.

However, the thinnest laminates show a marked decrease in impact duration until fibre damage occurs, even though delamination was present. This is because of the non-linear membrane effect not allowed for in equation (12). Tests on thin specimens at higher impact energies lead to higher deflections and hence membrane effects which increase stiffness and thus reduce impact durations. This reduction in duration could also be in part due to strain-rate dependence of material properties (Zhou and Davies 1995, Hancox and Mayer 1993) since as incident energy is increased the maximum deflection increases whilst the duration reduces giving an increase in strain rate. However, since a similar effect was not seen for thicker specimens any such effects are not thought to be significant.

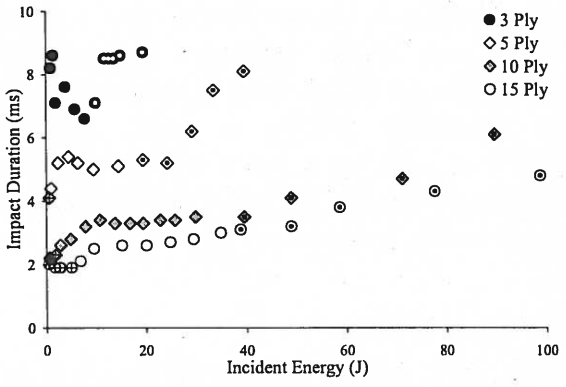

Figure 15: Impact Durations, 50mm Diameter Specimens

5 CONCLUSIONS

Drop-weight impact tests have been carried out for low fibre-volume glass-polyester laminates for two geometrically scaled circular specimen sizes and for a range of diameter to thickness ratios. The impact behaviour has been characterised as a progression of three damage stages with

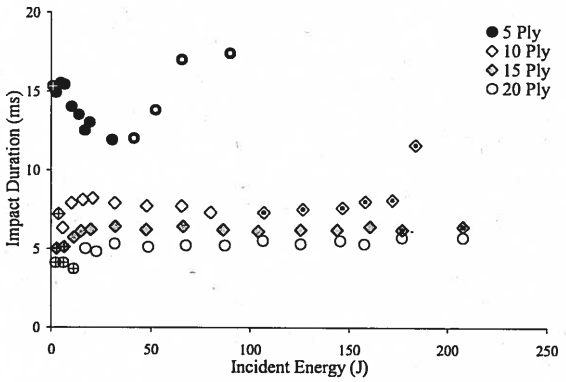

Figure 16: Impact Durations, 100mm Diameter Specimens

increasing incident energy, namely 'Un-delaminated', 'Delaminated' and 'Fibre damage'. The following points for the impact behaviour of marine composites have been concluded:

- Impact damage occurs in two main stages: hidden internal delamination damage at low incident energy, and then at high incident energies perforation failure. Hence, high strain to failure reinforcement fibres will improve the perforation resistance, but good interlaminar shear properties are also required to resist and reduce delamination.
- Bending and membrane effects are significant for thin laminates. For thick laminates, especially after the sudden onset of delamination, the response is shear-dominated.
- A fracture mechanics model describes extremely well the sudden onset of internal delamination, and gives good scaling between specimen sizes.
- An energy balance approach gives good correlation between impact force and incident energy.
- Fibre failure leading to penetration is thought to be back-face tension controlled, although fibre shear-out may become important for very low diameter to thickness ratios.

6 ACNOWLEDGEMENTS

This work has been financed by Fundação para a Ciência e a Tecnologia, Lisbon, Portugal, through its pluri-annual funding awarded to the Unit of Marine Technology and Engineering. The first author has been financed by a scholarship from the Fundação para a Ciência e a Tecnologia, under contract number SFRH / BPD / 1568 / 2000.

7 REFERENCES

Abrate S. Impact on composite structures. Cambridge University Press, 1998.

Abrate S. Modelling of impacts on composite structures. Composite Structures; 51: 129-138, 2001.

Caprino G. and Lopresto V. On the penetration energy for fibre-reinforced plastics under low-velocity impact conditions. Composite Science and Technology; 61: 65-73, 2001.

Cartié D.D.R. and Irving P.E. Effect of resin and fibre properties on impact and compression after impact performance of CFRP. Composites Part A; 33: 483-493, 2002.

Chen J.K., Sun C.T. Dynamic large deflection response of composite laminate subject to impact. Composite Structures; 4(1): 59-73, 1985.

Christoforou A.P. Impact dynamics and damage in composite structures. Composite Structures; 52: 181-188, 2001.

Davies GAO. and Zhang X. Impact damage prediction in carbon composite structures. Int J Impact Eng; 16(1):149-170, 1995.

Davies GAO., Hitchings D. and Zhou G. Impact damage and residual strengths of woven fabric glass/polyester laminates. Composites Part A;27A:1147-1156, 1993.

Hancox, NL. and Mayer RM. Design Data for Reinforced Plastics. Chapman and Hall, 1993.

Hirai Y., Hamada H. and Kim J.K. Impact response of woven glass-fabric composites – I. Effect of fibre surface treatment. Composite Science and Technology; 58: 91-104, 1998.

Mouritz AP, Gellert E, Burchill P and Challis K. Review of advanced composite structures for naval ships and submarines. Composite Structures; 53:21-41, 2001.

Richardson M.O.W. and Wisheart M.J. Review of low-velocity impact properties of composite materials. Composites Part A; 27A: 1123-1131, 1996.

Shivakumar KN., Elber W. and Illg W. Prediction of impact force and duration due to low-velocity impact on circular composite laminates. J. Appl. Mech.;52:674-680, 1985.

Sun C.T., Dicken A., Wu H.F. Characterization of impact damage in ARALL laminates. Composite Science and Technology; 49: 139-144, 1993.

Sutherland L.S. and Guedes Soares C. Impact tests on woven roving e-glass/polyester laminates. Composites Science and Technology;59:1553-1567, 1999a.

Sutherland L.S. and Guedes Soares C. Effects of laminate thickness and reinforcement type on the impact behaviour of e-glass/polyester laminates. Composites Science and Technology; 59:2243-2260, 1999b.

Sutherland L.S., Machado Santos F. and Guedes Soares G. "Indentation of marine composites." 5º Encontro Nacional de Análise Experimental de Tensões e Mecânica Experimental, Universidade de Coimbra 21-23 January 2004

Sutherland LS. and Guedes Soares C. The effects of test parameters on the impact response of glass reinforced plastic using an experimental design approach. Composites Science and Technology; 63:1-18, 2003.

Tan TM. and Sun CT. Use of statical indentation laws in the impact analysis of laminated composite plates. Trans. ASME; 52:6-12, 1985.

Yang S.H., Sun C.T. Indentation law for composite laminates. ASTM STP 787: 425-449, 1982.

Zhou G, Davies GAO. Impact response of thick glass fibre reinforced polyester laminates. Int J Impact Eng; 16(3):357-374, 1995.